

Free-space optical two-way time and frequency transfer compatible with current microwave satellite transfer platform

HONGLEI YANG,^{1,2,3,*} HAIFENG WANG,^{1,3} HANG YI,¹ XUEYUN WANG,¹
HONGBO WANG,¹ AND SHENGLANG ZHANG¹

¹ *Science and Technology on Metrology and Calibration Laboratory, Beijing Institute of Radio Metrology and Measurement, Beijing 100854, China*

² *State Key Laboratory of Precision Measurement Technology & Instruments, Department of Precision Instrument, Tsinghua University, Beijing 100084, China*

³ *These authors equally contributed to this work.*

*yhlpc@163.com

Abstract: Free-space optical two-way time and frequency transfer (O-TWTFT) has shown higher precision than microwave-band transfer methods and more flexibility compared to fiber-based techniques. Here we propose a free-space O-TWTFT system using flexible binary offset carrier modulation. The alternative method, compared with the BPSK-based O-TWTFT in [Optica **5**, 1542 (2018)], is totally compatible with the microwave satellite transfer equipment, and further reduces at least 95% occupied bandwidth to allow for expanding access capacity. We demonstrated time and frequency transfer between two sites separated by an outdoor path of 30 m with our home-built system. During a 15-hour transfer, the fractional frequency instability exhibits 4.0×10^{-12} at a gate time of 1 s, and approaches to 2.6×10^{-15} at 10000 s. The time deviation is 2.3 ps in a 1-s averaging time, and averages down to 1.0 ps until ~60 s. The method could be applicable to near-future ground-to-satellite/inter-satellite clock networks and outdoor timing services.

© 2019 Optical Society of America under the terms of the [OSA Open Access Publishing Agreement](#)

1. Introduction

Nowadays, positioning, navigation and timing (PNT) capabilities and technologies have been promoting rapid developments in diverse fields, such as civilian activity, financial trade, transportation management, electric power dispatch, logistics, etc. Among these technologies, timing service lays a solid foundation of the others. In recent years, the performance of optical atomic clock has been endlessly updated and achieves an unprecedented instability and accuracy at a level of 10^{-18} , which exceedingly satisfies the aforementioned applications [2,3]. Therefore, time and frequency transfer becomes the bottleneck of timing service.

Conventional methods of time and frequency transfer are based on free-space microwave telecommunication through geostationary (GEO) telecommunication satellites, typically referred to as two-way satellite time and frequency transfer (TWSTFT), and global navigation satellite systems (GNSS) [4]. By simultaneously sending and receiving microwave signals between a pair of exchange stations through an intermediate GEO satellite, common effect in one-way path could be almost cancelled out. This facilitates the time transfer instability to reach a few parts in 10^{11} in 1 s [5]. The GNSS method is more simple to operate, but at the cost of poor instantaneity and lower stability [6,7].

More precision methods have been explored in optical domain, where supports better accuracy, higher stability and boarder bandwidth. Although fiber networks could realize time transfer via microwave modulation between time-keeping laboratories [8] and frequency transfer via fiber noise cancellation between remote state-of-the-art narrow-linewidth lasers [9-11]. Less flexibility and costlier establishment are the drawbacks compared to free-space approaches. Analogue to fiber noise cancellation, free-space phase compensations over ~100

m distances, in either comb-based frequency transfer [12-14] or optical-carrier-based frequency transfer [15,16], have resulted in an instability better than 1×10^{-13} in 1 s. The inherent lack of time information restricts timing service. Recently, comb-based optical two-way time and frequency transfer (O-TWTFT) over a 2-km free-space link has demonstrated femtosecond level synchronization via time-of-flight method [17-20], and further achieved attosecond level transfer with carrier phase method, at which is capable to frequency comparison between optical atomic clocks without fiber link [21]. Nevertheless, the high precision is not always required in general applications. Free-space O-TWTFT with digital coherent communication has reached sub-picosecond timing precision across a 4-km turbulent range [1]. Besides, several ground-to-satellite projects, such as time transfer by laser link (T2L2) and European laser timing (ELT), have realized picosecond level transfer [22,23].

Here we propose an alternative picosecond-level free-space O-TWTFT using flexible binary offset carrier (FlexBOC) modulation based on spread-spectrum microwave satellite technique, thus is completely compatible with practical TWSTFT systems. The adoption of FlexBOC modulation reduces at least 95 % occupied bandwidth compared to binary phase-shift keyed (BPSK) modulation [1], but yields comparative precision due to comprehensive analysis between the code and sub-carrier in FlexBOC signal. Moreover, the time interval measurement avoids a continuous link that may be routinely broken by physical obstructions.

2. Experimental Setup

Figure 1(a) shows the free-space O-TWTFT layout based on FlexBOC modulation. Sites A and B are co-located but not necessarily to share the identical Rubidium frequency standard for the convenience of verification. Each FlexBOC transceiver fulfills both pseudo ranging and data interaction in full duplex mode, such that the encoded C-band continuous-wave laser lights are simultaneously transferred across a 30-m free-space outdoor path in both directions. The reciprocity of the atmosphere is fully exploited to suppress the routine environmental turbulence along the traversing path [24].

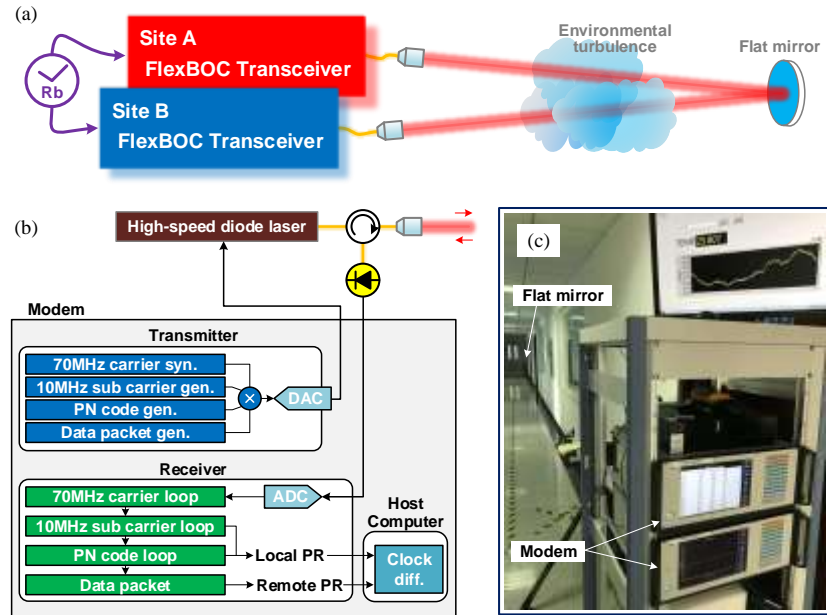


Fig. 1. (a) Schematic of the free-space O-TWTFT system based on FlexBOC modulation. (b) Top-level design of the FlexBOC transceiver. (c) Snapshot of the experimental system. syn, synthesizer; gen, generator; ADC, analog-to-digital converter; DAC, digital-to-analog converter; PN, pseudorandom noise; PR, pseudo range; Clock diff, Clock difference.

Figure 1(b) illustrates the schematic of the transceiver and the modem is described in Ref. [25]. Individual diode lasers emit 4-mW optical carriers at ~ 1550 nm and are capable to current modulation with a broad bandwidth up to ~ 3 GHz. The encoded optical carriers according to the FlexBOC signal generated by the modem are collimated at local site, and reciprocally transmitted to the opposite site in free space. To enhance the reciprocity of the link, the differential length variations of fiber-coupled circulators are minimized by passive temperature control. The received light is decoded by digital phase-lock loops for pseudo range measurement and data extraction. The host computer records one-way pseudo range along both directions and calculates clock time difference every second. Figure 1(c) exhibits the snapshot of the experimental setup.

Within the transmitter of the modem, the generated FlexBOC signal contains four components. A 70-MHz intermediate frequency (IF) signal is synthesized to shift the modulation from the optical carrier. A 10-MHz sub-carrier is added for fine pseudo ranging. A unique pseudorandom noise (PN) code is used for coarse pseudo ranging and transceiver identification as well. One PN code sequence contains 125 chips with $8 \mu\text{s}$ chip duration (125 kHz chip rate). Therefore, PN code sequences regenerate every 1 ms and enables clock time difference measurement at a maximum rate of 1 kHz. Pseudo range including other interactive data are combined as digital codes for date exchange between individual sites. The four signal components are mixed together in time domain, and then used to modulate the driving current of high-speed diode laser.

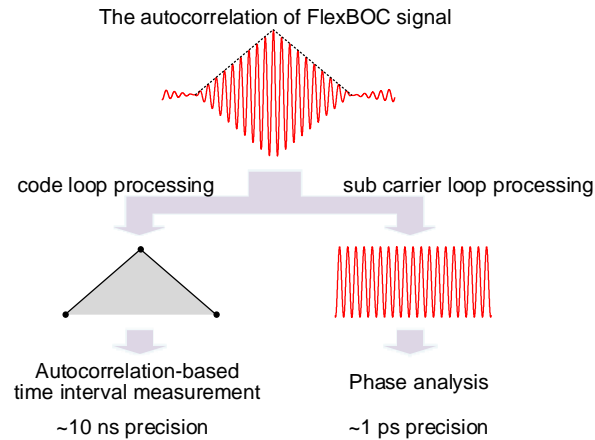


Fig. 2. Methodology of local pseudo ranging via FlexBOC signal.

In the receiver of the modem, both time interval measurement with autocorrelation and carrier phase analysis are utilized in order to realize local pseudo ranging. The methodology is interpreted in Fig. 2. The autocorrelation of the FlexBOC signal is a center-burst with inner carrier. The triangular envelop is generated by the PN codes, while the inner carrier is from the fundamental component of the square sub-carrier. Practically, resolving and tracking the autocorrelation signal significantly burdens computational overhead, and complicates processing algorithm. Instead, we plant three digital phase-lock loops to extract the signal components in turns, i.e., the 70-MHz IF carrier, 10-MHz square sub-carrier, PN code and interactive data. Then, the PN code and sub-carrier are separately resolved and tracked in parallel. The autocorrelation-based time interval measurement of the PN code provides a ~ 10 -ns precision for coarse pseudo ranging, which is below the sampling period of 17 ns, while the phase analysis of the sub-carrier could further enhance to picosecond-level precision. Eventually, the clock time difference is found in the host computer every second with local pseudo range and remote pseudo range translated from the interactive data.

Note that the sub-carrier is generated as a square waveform in a digital way, which inherits the conventional BOC scheme [26]. Nevertheless, the high-order harmonics (the remaining fundamental wave for the phase analysis) are filtered out in the processing with a benefit of dramatically releasing the occupied bandwidth in one link configuration. The typical bandwidth of the sub-carrier principal lobe is 500 kHz, which owns 2.5 % bandwidth between the two sub-carrier peaks, as depicted in Fig. 3. When compared to BPSK modulation, i.e., 10 MHz chip rate [1], this method also provides a bandwidth release at least 95 %. Meanwhile, the frequency of sub-carrier is capable to agile configuration. The improved design could hold a highly efficient multi-link expandability, but also increase the applicability when the bandwidth resource of a satellite is in high duty and dense assignment.

Figure 3 exhibits typical RF spectra of the FlexBOC signals in the modem. Although there is a ~40-dB loss between the transmitter and receiver, picosecond-level transfer still maintained for a long period. Actually, even if the received FlexBOC signal was submerged in the noise floor, it could be extracted due to the autocorrelation procession in the signal recovery of spread-spectrum communication. Hence we estimate the minimum output power of the transmitter to be around -40 dBm over a 30-m link.

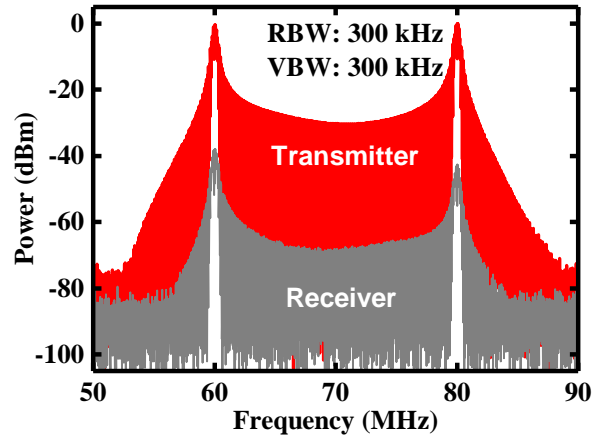


Fig. 3. Typical RF spectra of the FlexBOC signals in the transmitter and receiver.

3. Results

Over a 30-m outdoor link, the time delay drifts of forward and backward pseudo range are depicted in Fig.4(a) and 4(b), respectively, and in a high agreement with ambient temperature variation during a 15-hour transfer. Small asymmetry of the both drifts was probably caused by differential time delays of fibers, cables and temperature-sensitive devices. Because of environmental turbulence across the free-space link, the peak-to-peak drifts were ~170 ps. According to two-way transfer methodology, this environmental effect could be cancelled out in the assumption of the reciprocity of atmosphere. The clock time difference is shown in Fig.4(c). The peak-to-peak value was reduced to 95 ps. Due to the aforementioned differential time delays, the clock time difference still changed following the temperature variation. The carrier-to-noise ratios were simultaneously recorded and shown in Fig. 4(d). Their variations also coincided with the temperature change. We next analyze the performance metrics in terms of Allan deviations in both time and frequency viewpoints.

The fractional frequency instability is given by the modified Allan deviation and exhibited in Fig. 5(a) for the data in Fig. 4(b). It reaches 4.0×10^{-12} at a gate time of 1 s, which is very closed to the performance of the frequency reference, and averages down as τ^{-1} until ~60 s. At 10000 s, the frequency transfer instability approaches to 2.6×10^{-15} . The time transfer stability is shown in Fig. 5(b) for the same data in Fig. 5(a). The time deviation within a 1-s averaging time is 2.3 ps. It drops to 1.0 ps until ~60 s and then reaches a floor, which approaches to the

limit [27]. It is clear to see that the time deviation above 60 s slows down the falling slope of frequency transfer instability. We could almost attribute the time deviation drift in a longer measurement interval to the differential time delays, which could be reduced by tighter temperature control of the fibers, cables and transceivers.

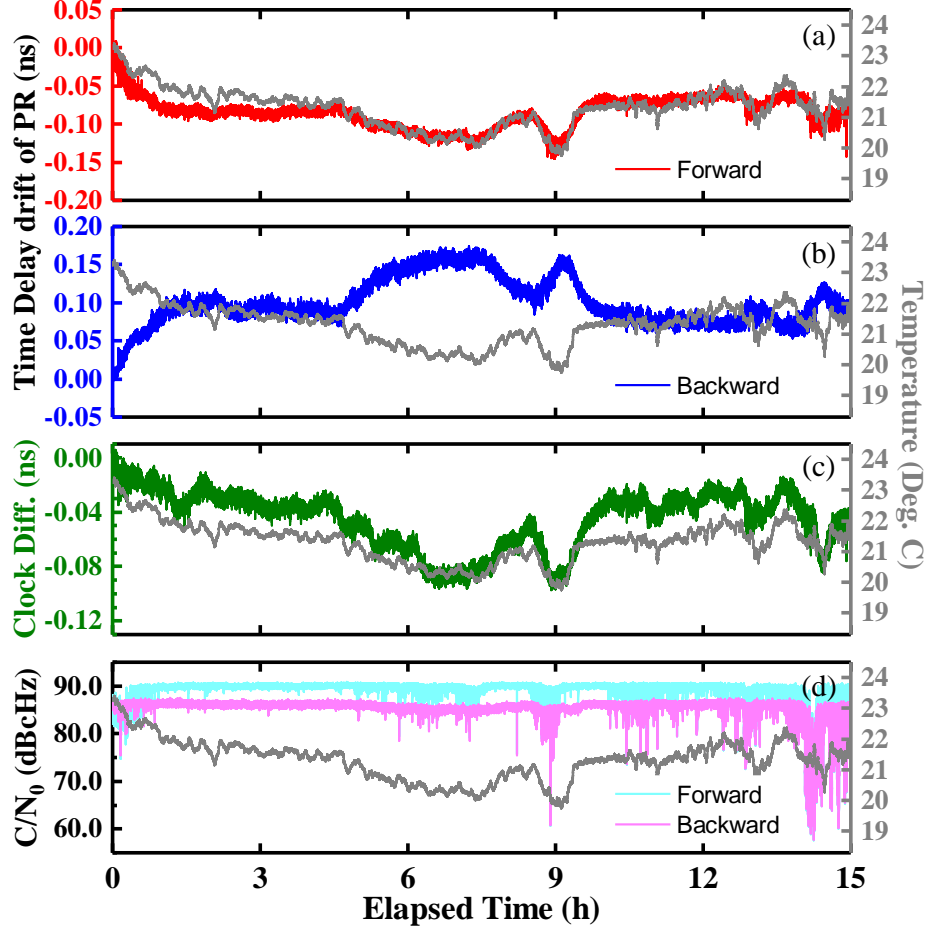


Fig. 4. (a) and (b) show the time delay drifts of pseudo range during a 15-h transfer in forward and backward directions, respectively. (c) Clock time difference. (d) Carrier-to-noise ratio. Ambient temperature was drawn in each subplot for clear view. PR, pseudo range; Clock diff, Clock difference; C/N_0 , carrier-to-noise ratio.

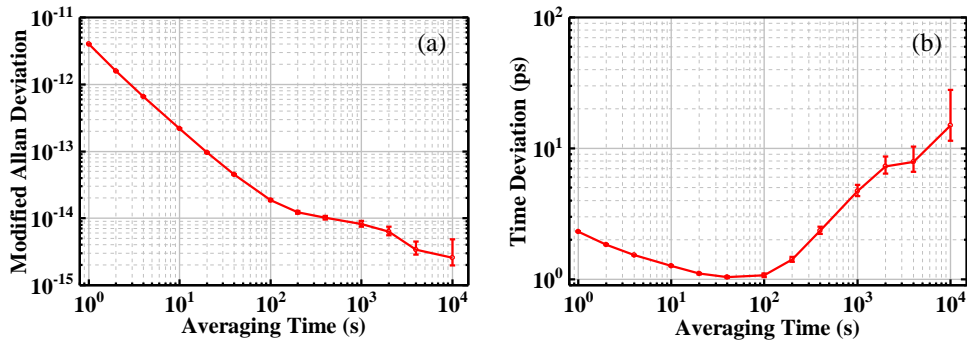


Fig. 5. (a) Modified Allan deviation and (b) Time deviation across a 30-m path.

4. Outlooks and discussion

In general, we have already demonstrated our alternative free-space optical two-way time and frequency transfer method via FlexBOC modulation. As other two-way time and frequency transfer techniques, our method also basically relied on the reciprocity of the link. The factors of the reciprocity have been clearly explained in several literatures [1,28], and are valid in our method as well. Here we briefly discuss the other performance limits, and illuminate some improvements in future.

In the current demonstration, we utilized an external Rubidium frequency standard as the common reference. The synthetic signals output from the transmitter and the test units in the receiver inherit the performance of the frequency standard. Right now, the time and frequency transfer performance metrics are very closed to the Rubidium frequency reference. Therefore, a better performance would be expected if a higher-stability reference was employed, such as a Hydrogen maser or photonic microwave divided down from a state-of-the-art cavity-stabilized laser according to Ref. [1], since the limit precision at such a high carrier-to-noise ratio shown in Fig. 4(d) is around 0.8 ps [27].

Noise from the current-modulated diode lasers is another limit because of tiny carrier frequency shift, therefore amplitude fluctuation when modulating the driving current around operating point. Amplitude-to-phase conversion would degrade the resolved phase of the sub-carrier for fine pseudo ranging. An electro-optical modulator could be inserted following the diode laser to achieve external phase modulation, instead of the driving-current modulation. In this scheme, coherent heterodyne detection is enabled to achieve higher-precision pseudo ranging [1,18].

For our system, the transfer could be recovered from active jamming by applying clock time difference measurement. However, beam alignment excursions resulted from environmental variation could break the transfer link irreversibly. Steering tip-tilt mirrors are essential for real-time compensation of mechanical creep due to environmental change [29], which leads to the drastic fluctuation of carrier-to-noise ratio at the end of demo in Fig. 4(d).

In addition, telescope terminal is also crucial when traversing range is scaled up to several kilometers, and even ground-to-satellite distance. In our demonstration, two commercialized free-space collimators were utilized as both input and output terminals. The insert losses were ~ 10 dB since the demo path length of 30 m was far beyond the nominal working distance (~ 6 m). We have designed a pair of telescope terminals with a larger diameter to expand the light beams for suppressing beam divergence, and as well to enlarge the receiving cross-section for high power-receiving efficiency.

Multi-link expandability should be highlighted, such that optical clock networks could be simply established and expanded by labeling unique PN code on individual modems. The capacity of access users is theoretically determined by the code size, and could be expanded by at least 20 fold according to the aforementioned bandwidth release. However, with increasing access users, the precision of pseudo ranging in each channel should be traded off because the noise-like FlexBOC signals in other links raise the noise floor of the local link. This phenomenon has been observed in our multi-link trial.

5. Conclusion

We have demonstrated a free-space O-TWTFT system using FlexBOC modulation compatible with microwave satellite transfer platform. At 30 m across an outdoor path during a 15-h period, our home-built system yields a time deviation of 2.3 ps at a gate time of 1 s, and averages down to 1.0 ps until ~ 60 s. The fractional frequency instability is 4.0×10^{-12} at 1 s, and approaches to 2.6×10^{-15} at 10000 s.

As discussed above, this approach could totally transplant into the current microwave satellite time and frequency transfer equipment, and further reduces 95 % occupied bandwidth to expand access capacity with a comparative precision. Meanwhile, the improved design of the modem could flexibly accommodate the real operation situation of the employed satellite

or other ground-based transponder. The method could be applicable to near-future ground-to-satellite/inter-satellite clock networks and outdoor timing services.

Funding

This work was partly supported by the Open Research Fund of the State Key Laboratory of Precision Measurement Technology and Instruments (Grant No. DL18-02).

References

1. I. Khader, H. Bergeron, L. C. Sinclair, W. C. Swann, N. R. Newbury, and J.-D. Deschênes, "Time synchronization over a free-space optical communication channel," *Optica* **5**, 1542-1548 (2018).
2. E. Oelker, R. B. Hutson, C. J. Kennedy, L. Sonderhouse, T. Bothwell, A. Goban, D. Kedar, C. Sanner, J. M. Robinson, G. E. Marti, D. G. Matei, T. Legero, M. Giunta, R. Holzwarth, F. Riehle, U. Sterr, and J. Ye, "Optical clock intercomparison with 6×10^{-19} precision in one hour," arXiv:1902.02741 (2019).
3. W. F. McGrew, X. Zhang, R. J. Fasano, S. A. Schäffer, K. Beloy, D. Nicolodi, R. C. Brown, N. Hinkley, G. Milani, M. Schioppa, T. H. Yoon, and A. D. Ludlow, "Atomic clock performance enabling geodesy below the centimetre level," *Nature* **564**, 87-90 (2018).
4. J. Levine, "A review of time and frequency transfer methods," *Metrologia* **45**, S162-S174 (2008).
5. M. Fujieda, D. Piester, T. Gotoh, J. Becker, M. Aida, and A. Bauch, "Carrier-phase two-way satellite frequency transfer over a very long baseline," *Metrologia* **51**, 253-262 (2014).
6. S. Droste, C. Grebing, J. Leute, S. M. F. Raupach, A. Matveev, T. W. Hänsch, A. Bauch, R. Holzwarth and G. Grosche, "Characterization of a 450km baseline GPS carrier-phase link using an optical fiber link," *New J. Phys.* **17** 083044 (2015).
7. M. Fujieda, S.-H. Yang, T. Gotoh, S.-W. Hwang, H. Hachisu, H. Kim, Y. K. Lee, R. Tabuchi, T. Ido, W.-K. Lee, M.-S. Heo, C. Y. Park, D.-H. Yu, and G. Petit, "Advanced Satellite-Based Frequency Transfer at the 10^{-16} Level," *IEEE Trans. Ultrason. Ferroelectr. Freq. Control* **65**, 973-978 (2018).
8. B. Wang, X. Zhu, C. Gao, Y. Bai, J. W. Dong, and L. J. Wang, "Square Kilometre Array Telescope—precision reference frequency synchronization via 1f-2f dissemination," *Sci. Rep.* **5**, 13851 (2015).
9. L.-S. Ma, P. Jungner, J. Ye, and J. L. Hall, "Delivering the same optical frequency at two places: accurate cancellation of phase noise introduced by an optical fiber or other time-varying path," *Opt. Lett.* **19**, 1777-1779 (1994).
10. K. Predehl, G. Grosche, S. M. F. Raupach, S. Droste, O. Terra, J. Alnis, T. Legero, T. W. Hänsch, T. Udem, R. Holzwarth, and H. Schnatz, "A 920-kilometer optical fiber link for frequency metrology at the 19th decimal place," *Science* **336**, 441-444 (2012).
11. S. Droste, F. Ozimek, T. Udem, K. Predehl, T. W. Hänsch, H. Schnatz, G. Grosche, and R. Holzwarth, "Optical-frequency transfer over a single-span 1840 km fiber link," *Phys. Rev. Lett.* **111**, 110801 (2013).
12. B. Ning, S. Y. Zhang, D. Hou, J. T. Wu, Z. B. Li, and J. Y. Zhao, "High-Precision Distribution of Highly Stable Optical Pulse Trains with 8.8×10^{-19} Instability," *Sci. Rep.* **4**, 5109 (2014).
13. F. Sun, D. Hou, D. Zhang, J. Tian, J. Hu, X. Huang, and S. Chen, "Femtosecond-level timing fluctuation suppression in atmospheric frequency transfer with passive phase conjunction correction," *Opt. Express* **25**(18):21312-21320 (2017).
14. H. J. Kang, B. J. Chun, J. Yang, Y. Kim, and S. Kim, "Comb-based Optical Frequency Transfer in Free Space," in Conference on Lasers and Electro-Optics, OSA Technical Digest (online), paper STh4L.5 (2017).
15. S. Chen, F. Sun, Q. Bai, D. Chen, Q. Chen, and D. Hou, "Sub-picosecond timing fluctuation suppression in laser-based atmospheric transfer of microwave signal using electronic phase compensation," *Opt. Commun.* **401**, 18-22 (2017).
16. Y. He, K. G. H. Baldwin, B. J. Orr, R. B. Warrington, M. J. Wouters, A. N. Luiten, P. Mirtschin, T. Tzioumis, C. Phillips, J. Stevens, B. Lennon, S. Munting, G. Aben, T. Newlands, and T. Rayner, "Long-distance telecom-fiber transfer of a radio-frequency reference for radio astronomy," *Optica* **5**, 138-146 (2018).
17. F. R. Giorgetta, W. C. Swann, L. C. Sinclair, E. Baumann, I. Coddington, and N. R. Newbury, "Optical Two-Way Time and Frequency Transfer over Free Space," *Nat. Photonics* **7**, 434 (2013).
18. J.-D. Deschênes, L. C. Sinclair, F. R. Giorgetta, W. C. Swann, E. Baumann, H. Bergeron, M. Cermak, I. Coddington, and N. R. Newbury, "Synchronization of distant optical clocks at the femtosecond level," *Phys. Rev. X* **6**, 021016 (2016).
19. H. Bergeron, L. C. Sinclair, W. C. Swann, I. Khader, K. C. Cossel, M. Cermak, J.-D. Deschênes, and N. R. Newbury, "Femtosecond synchronization of optical clocks off of a flying quadcopter," arXiv:1808.07870 (2018).
20. H. Zhang, H. Wei, H. Yang, and Y. Li, "Active laser ranging with frequency transfer using frequency comb," *Appl. Phys. Lett.* **108**, 181101 (2016).
21. L. C. Sinclair, H. Bergeron, W. C. Swann, E. Baumann, J.-D. Deschênes, and N. R. Newbury, "Comparing optical oscillators across the air to milliradians in phase and 10^{-17} in frequency," *Phys. Rev. Lett.* **120**, 050801 (2018).
22. K. U. Schreiber, I. Prochazka, P. Lauber, U. Hugentobler, W. Schafer, L. Cacciapuoti, and R. Nasca, "Ground-based demonstration of the European laser timing (ELT) experiment," *IEEE Trans. Ultrason. Ferroelectr. Freq. Control* **57**, 728-737 (2010).

23. E. Samain, P. Exertier, P. Guillemot, P. Laurent, F. Pierron, D. Rovera, J. Torre, M. Abgrall, J. Achkar, D. Albanese, C. Courde, K. Djeroud, M. L. Bourez, S. Leon, H. Mariey, G. Martinot-Lagarde, J. L. Oneto, J. Paris, M. Pierron, and H. Viot, "Time transfer by laser link-T2L2: current status and future experiments," in Joint Conference of the IEEE International Frequency Control and the European Frequency and Time Forum (IFCS/EFTF), pp1-6 (2011).
24. D. Kirchner, "Two-way time transfer via communication satellites," *Proc. IEEE* **79**, 983-990 (1991).
25. H. Wang, X. Wang, H. Wang, H. Yi, S. Wang, W. Yang and S. Zhang, "Three loops - A method for tracking a new TWSTFT signal FBOC," in Joint Conference of the European Frequency and Time Forum and IEEE International Frequency Control Symposium (EFTF/IFCS), pp375-377 (2017).
26. J. W. Betz, "Binary Offset Carrier Modulations for Radionavigation," *Navigation* **48**(4): 227-246 (2001).
27. T. Gotoh, J. Amagai, T. Hobiger, M. Fujieda, and M. Aida, "Development of a GPU-Based Two-Way Time Transfer Modem," *IEEE Trans. Instrum. & Meas.*, **60**(7):2495-2499 (2011).
28. L. C. Sinclair, F. R. Giorgetta, W. C. Swann, E. Baumann, I. Coddington, and N. R. Newbury, "Optical Phase Noise from Atmospheric Fluctuations and Its Impact on Optical Time-Frequency Transfer," *Phys. Rev. A* **89**, 023805 (2014).
29. W. C. Swann, L. C. Sinclair, I. Khader, H. Bergeron, J.-D. Deschênes, and N. R. Newbury, "Low-loss reciprocal optical terminals for two-way time-frequency transfer," *Appl. Opt.* **56**(34): 9406-9413 (2017).